Lipid peroxidation and water penetration in lipid bilayers: A W-band EPR study

Conte, Elena; Megli, Francesco Maria; Khandelia, Himanshu; Jeschke, Gunnar; Bordignon, Enrica

How to cite

CONTE, Elena et al. Lipid peroxidation and water penetration in lipid bilayers: A W-band EPR study. In: Biochimica et biophysica acta. Biomembranes, 2013, vol. 1828, n° 2, p. 510–517. doi: 10.1016/j.bbamem.2012.09.026

This publication URL: https://archive-ouverte.unige.ch/unige:173898

Publication DOI: 10.1016/j.bbamem.2012.09.026

Biochimica et Biophysica Acta 1828 (2013) 510–517

Contents lists available at SciVerse ScienceDirect

Biochimica et Biophysica Acta

journal homepage: www.elsevier.com/locate/bbamem

Lipid peroxidation and water penetration in lipid bilayers: A W-band EPR study

Elena Conte [a], Francesco Maria Megli [a], Himanshu Khandelia [b], Gunnar Jeschke [c], Enrica Bordignon [c,*]

[a] Centro di Studio sui Mitocondri e Metabolismo Energetico (CNR) c/o Dipartimento di Biochimica e Biologia Molecolare, Università di Bari, V. Orabona 4, 70126 Bari, Italy
[b] MEMPHYS, Center for BioMembrane Physics, University of Southern Denmark, Campusvej 55, Odense M 5230, Denmark
[c] ETH Zurich, Laboratory of Physical Chemistry, Wolfgang-Pauli-Strasse 10, 8093 Zurich, Switzerland

ARTICLE INFO

Article history:
Received 17 July 2012
Received in revised form 24 September 2012
Accepted 25 September 2012
Available online 1 October 2012

Keywords:
Phospholipid bilayer
Lipoperoxidation
Spin labeling
W-band EPR
Bilayer polarity
Molecular dynamics

ABSTRACT

Lipid peroxidation plays a key role in the alteration of cell membrane's properties. Here we used as model systems multilamellar vesicles (MLVs) made of the first two products in the oxidative cascade of linoleoyl lecithin, namely 1-palmitoyl-2-(13-hydroperoxy-9,11-octadecanedienoyl)-lecithin (HpPLPC) and 1-palmitoyl-2-(13-hydroxy-9,11-octadecanedienoyl)-lecithin (OHPLPC), exhibiting a hydroperoxide or a hydroxy group at position 13, respectively. The two oxidized lipids were used either pure or in a 1:1 molar ratio mixture with untreated 1-palmitoyl-2-linoleoyl-lecithin (PLPC). The model membranes were doped with spin-labeled lipids to study bilayer alterations by electron paramagnetic resonance (EPR) spectroscopy. Two different spin-labeled lipids were used, bearing the doxyl ring at position (n) 5 or 16: γ-palmitoyl-β-(n-doxylstearoyl)-lecithin (n-DSPPC) and n-doxylstearic acid (n-DSA). Small changes in the acyl chain order in the sub-polar region and at the methyl-terminal induced by lipid peroxidation were detected by X-band EPR. Concomitantly, the polarity and proticity of the membrane bilayer in those regions were investigated at W band in frozen samples. Analysis of the g_{xx} and A_{zz} parameters revealed that OHPLPC, but mostly HpPLPC, induced a measurable increase in polarity and H-bonding propensity in the central region of the bilayer. Molecular dynamics simulation performed on 16-DSA in the PLPC–HpPLPC bilayer revealed that water molecules are statistically favored with respect to the hydroperoxide groups to interact with the nitroxide at the methyl-terminal, confirming that the H-bonds experimentally observed are due to increased water penetration in the bilayer. The EPR and MD data on model membranes demonstrate that cell membrane damage by oxidative stress cause alteration of water penetration in the bilayer.

1. Introduction

Cell membranes are made of a specific mixture of proteins and lipids representing the basic structural component of various organs and organelles such as mitochondria and chloroplasts. Membranes play a crucial role in many cellular processes. Oxidative stress in the cells occurring as a consequence of an inequity between the pro-oxidant/antioxidant systems, causes injury to biomolecules such as nucleic acids, proteins, structural carbohydrates, and lipids [1]. Oxidized phospholipids are characterized by the presence of variously oxygenated and oxidatively modified fatty residues, highly unusual in the ordered bilayer hydrophobic core. To date, lipid peroxidation is increasingly considered as a deleterious process that can perturb the bilayer structure leading to modifications of basic properties such as the ordering of fatty acid chains [2], lateral phase separation [3], phase transition temperature [4], reversal of truncated acyl chains into the outer water medium [5–7], accompanied by variations of lateral diffusion and chain mobility [8]. A concomitant increase of water penetration in peroxidized bilayers [8–10] and a facilitated phospholipid flip-flop have been observed [11]. The bilayer alterations are thought to impact heavily onto membrane functioning so that changes in a variety of biological processes can be expected, leading to pathological implications [12,13].

Lipid peroxides derive from ROS (reactive oxygen species) and RNS (reactive nitrogen species) attack the polyunsaturated fatty acids. The first stable intermediates of lipid peroxidation are hydroperoxy- and hydroxy-conjugate dienes. Natural membranes are characterized by the existence of lipid microdomains with different phospholipid composition and unsaturation degree. Following ROS attack, fully unsaturated microdomains could well turn into fully oxidized microdomains, though representing a small percentage of the whole lipidome. Furthermore, no typical oxidation pattern has ever been defined for any natural peroxidized membrane, or can be defined at the present state of knowledge, since oxidative stress strikes in a still unknown variety of pathways, ending in a still non-understood variety

Abbreviations: 105-DSPPC, 1-palmitoyl-2-(5-doxylstearoyl)-lecithin; 16-DSPPC, 1-palmitoyl-2-(16-doxylstearoyl)-lecithin; 5-DSA, 5-doxylstearic acid; 16-DSA, 16-doxylstearic acid; EPR, electron paramagnetic resonance; HpPLPC, 1-palmitoyl-2-(13-hydroperoxy-9,11-octadecanedienoyl)-lecithin; MLV, multilamellar vesicles; OHPLPC, 1-palmitoyl-2-(13-hydroxy-9,11-octadecanedienoyl)-lecithin; PLPC, 1-palmitoyl-2-linoleoyl-lecithin; ROS, reactive oxygen species

* Corresponding author. Tel.: +41 44 6337570; fax: +41 44 6331448.
E-mail address: enrica.bordignon@phys.chem.ethz.ch (E. Bordignon).

0005-2736/$ – see front matter © 2012 Elsevier B.V. All rights reserved.
http://dx.doi.org/10.1016/j.bbamem.2012.09.026

of oxidation patterns, depending on the oxidizing agent and the oxidation conditions, or the type of oxidative pathology. Mass spectrometry studies of oxidative lipidomics in pathological tissues can help to address those issues [14,15]. Following these considerations, natural lipoperoxidized membrane composition cannot be precisely defined, while characterization of model membrane enriched in the species of interest can give first insights into the general effects of oxidative stress on the bilayer properties. In this study we focused on the effects induced on model membranes formed by the normal species 1-palmitoyl-2-linoleoyl-sn-glycero-3-phosphatidylcholine (PLPC) by the introduction of the two leading intermediate species in lipid peroxidation, namely 1-palmitoyl-2-(13-hydroperoxy-9,11-octadecanedienoyl)-lecithin (HpPLPC) and 1-palmitoyl-2-(13-hydroxy-9,11-octadecanedienoyl)-lecithin (OHPLPC) in a 50 to 100% molar percentage (Fig. 1). Two different lipids carrying the doxyl spin labels at position (n) 5 or 16, namely γ-palmitoyl-β-(n-doxylstearoyl)-lecithin (n-DSPPC) and n-doxylstearic acid (n-DSA) (Fig. 1) will be used as reporter molecules for membrane polarity and acyl chain order at the sub-polar and methyl terminal regions of the bilayer. Fatty acid spin labels (n-DSA) are evenly distributed among the phospholipids, and spin-labeled lecithins (n-DSPPC) are integrated into the bilayer, thus they provide complementary measures of the amplitude of motion of the molecular long axis about the average orientation of the fatty acid chain in the lipid bilayer.

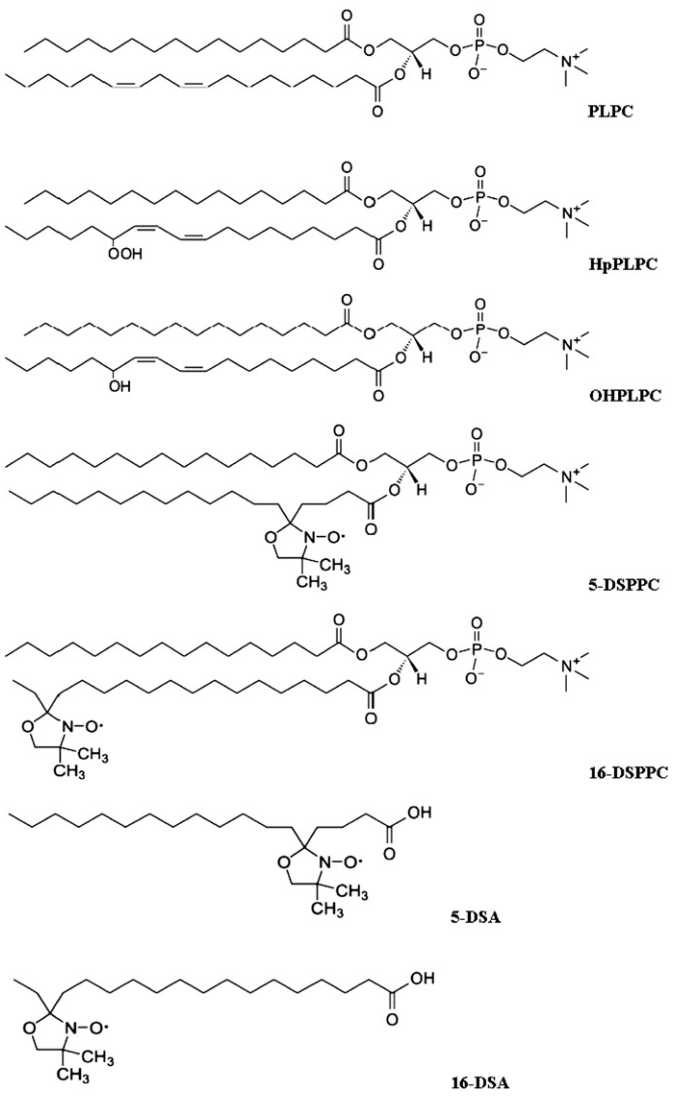

Fig. 1. Chemical structures of the spin labels and the oxidized phospholipids used in this study.

Previously, EPR was used to study alteration of the acyl chain order upon lipid peroxidation using various n-doxyl stearate spin probes [16]. X-band EPR measurements were later performed on planar bilayers made of pure PLPC, pure HpPLPC or a PLPC/HpPLPC 1:1 mixture in order to explore the effects on the phospholipid bilayer geometrical order [17]. It was found that conjugated-dienes lecithins did not alter fatty acid chain alignment in the bilayer hydrophobic interior. In a subsequent study [4], X-band EPR measurements were performed on multilamellar vesicles (MLVs) made of PLPC, HpPLPC, and OHPLPC either pure or mixed in order to study the effects on lateral phase separation, gel–solid to gel–liquid transition temperature, polarity and acyl chain order. It was concluded that OHPLPC/PLPC and HpPLPC/PLPC MLVs featured lateral phase separation at room temperature and gel–solid to gel–liquid transition temperature values are lower than pure those of PLPC MLVs. Although MD simulations suggested that the presence of polar oxygenated groups into the lipid bilayer could increase water penetration [8,9], the polarity profile experimentally obtained from the isotropic hyperfine value extracted from high temperature (60–80 °C) continuous wave EPR spectra was similar to that obtained for non-oxidized PLPC MLVs [4]. In this study, we investigate by high frequency EPR at cryogenic temperature the suggested change in water penetration upon lipid peroxidation. The W-band data reveal changes in polarity and proticity in the phospholipid bilayer upon lipid peroxidation, proving the insufficient sensitivity of the high temperature X-band EPR method applied before. The heterogeneous g_{xx} spectral region detected for the spin label at position 16 in both DSA and DSPPC allowed a detailed inspection of the changes in the H-bonding to the nitroxide group upon lipid peroxidation, which are attributed to changes in the water content in the middle of the bilayer on the basis of molecular dynamics simulation.

2. Materials and methods

2.1. Materials

5-doxylstearic acid (5-DSA), 16-doxylstearic acid (16-DSA) and lipoxidase (type V from soybean, EC 1.13.11.12) were purchased from Sigma; 1-palmitoyl-2-linoleoyl-glycero-3-phosphocholine (PLPC) was supplied by Avanti Polar Lipids; solvents were Baker HPLC grade. Lichroprep RP18 (40–63 μm) silica gel was from Merck.

2.2. Phospholipid modification

1 γ-palmitoyl—β-(n-doxylstearoyl)-lecithin (5- or 16-DSPPC) was obtained by coupling n-doxylstearic acid (n-DSA) to 1-palmitoyl-2-lyso-lecithin according to Boss et al. [18], and purified by reverse-phase (RP-18 silica gel) flash-chromatography followed by an elution UV–VIS spectrophotometer (Cary 50) with a continuous flow quartz cuvette (Hellma) at a wavelength of 235 nm [17]. 1-palmitoyl-2-(13-hydroperoxy-9,11-octadecanedienoyl)-lecithin (HpPLPC) was obtained by action of lipoxidase on PLPC [19]. The molecular structure of the product was confirmed by mass spectrometry. The mass spectrum and the fragmentation mechanism of the molecule confirming the C-13 hydroperoxide group position are given Fig. S1. In this context, we point out that numbering of the –OOH group at position C-9 cited in [4,20] was erroneous, and that the correct structure of the molecule used for those measurements is the one shown in [17] and in this work (Fig. 1). Reduction of these species with $NaBH_4$ yielded 1-palmitoyl-2-(13-hydroxy-9,11-octadecanedienoyl)-lecithin (OHPLPC). After extraction from the reaction mixture by the method of Bligh and Dyer [21], the products were purified by RP18 silica gel reverse-phase preparative column

flash-chromatography, using $CH_3OH/(C_2H_5)_2O/H_2O$ 95:5:2 (vol). Quantitative phosphorus analysis was performed according to [22].

2.3. Vesicles preparation

Vesicles (MLVs) were prepared according to Marsh et al. [23]. MLVs were chosen for this study for their well-defined thermal behavior and the similarly relaxed curvature in both leaflets. Briefly, the desired phospholipid mixture was dissolved in 0.5 ml dichloromethane and dried to a thin film under a nitrogen stream in a test tube at 40 °C. After further drying for 30 min under vacuum, the film was hydrated with 0.5 ml of a 100 mM KCl, 10 mM Tris/HCl, pH 8 buffer for 20 min at 40 °C. For EPR measurements, 2% (by mol) of the desired spin-labeled (5- or 16-doxylstearoyl-phosphatidylcholine; 5- or 16-doxylstearic acid), was included in the initial mixture and the hydrated preparation was concentrated to 10 μl after centrifuging for 30 min at 10,000 *g* in a 5417R refrigerated centrifuge.

Spin-labeled MLVs (1–2 μl) were then transferred to a quartz capillary (0.89 mm outer diameter, 0.5 mm inner diameter) at room temperature and snap frozen in a big reservoir of liquid nitrogen before insertion in the W-band resonator pre-cooled at 160 K. The small diameter of the capillary allows for extremely fast freezing times. The same quartz capillaries were also placed in a 3.8 mm quartz tube, and room temperature X-band spectra were detected before and after the W-band measurements in order to verify the absence of membrane damage after freezing/thawing. The MLVs containing HpPLPC, species known to be unstable over time, were prepared and directly measured within 1–2 days after the lipid preparation.

2.4. Polarity and proticity determination: W-band EPR

The low temperature (160 K) cw W-band EPR spectra (94.1–94.2 GHz) were recorded on a Bruker Elexsys E680 spectrometer equipped with a W-band probehead. Samples were loaded into W-band quartz capillaries and spectra were recorded with 5 μW microwave power, 100 kHz field modulation, 0.25 mT modulation amplitude, 400 Gauss sweep width, without automatic frequency control. Up to 8 spectra were averaged. The g_{xx} and A_{zz} values, diagnostic for polarity and water penetration into the membrane, were obtained by fitting of simulated spectra to the experimental ones. The simulated spectra were obtained with the Easyspin function "pepper" [24] using one or two different g_{xx} values corresponding to one or two nitroxide populations. The g_{xx} and A_{zz} parameters obtained from the fits are presented in Table S1.

2.5. Molecular dynamics simulations

Simulations were carried out with 2 molecules of 16-DSA randomly placed in each leaflet of a bilayer containing 62 molecules each of HpPLPC and PLPC. The modified Berger force field [25], with parameters adapted from http://moose.bio.ucalgary.ca/ was used for PLPC. Force field parameters for HpPLPC were the same as used in [9] and were kindly provided by Luca Monticelli. Force field parameters of 16-DSA were those used in [26], and kindly provided by Tomasz Rog. Water was represented by a single point charge (SPC) model [27]. The simulation was implemented in GROMACS package version 4.5.3 [28–30]. Simulation conditions and treatment of non-bonded parameters were similar to those reported in [31]. The system was simulated in the NPT ensemble for 200 ns at 310 K with a time step of 2 fs using a leap-frog integrator [32]. Temperature coupling was performed using the Nose-Hoover thermostat [33,34] with a reference temperature of 310 K. A semi-isotropic pressure coupling was applied using the Parinello–Rahman barostat [35] with a coupling constant of 0.1 ps and a reference pressure of 1.0 bar in all directions. The compressibility value for pure water, $4.5 \cdot 10^{-5}$ bar^{-1}, was used. Trajectories were sampled every 10 ps.

3. Results

3.1. Lipid peroxidation does not affect acyl chain order at room temperature

Spin-labeled 5- or 16-DSPPC and 5- or 16-DSA were used as reporter molecules at room temperature in MLVs prepared with pure PLPC, PLPC containing 50% of the corresponding conjugated-dienes lecithin, and pure HpPLPC or OHPLPC. The lipids used in this study have transition temperatures below 0 °C [4] (−18 °C for PLPC), thus they are fluid at room temperature. Spin-labeled lipids in fluid lipid membranes usually display axially anisotropic spectra, for which the ^{14}N-hyperfine anisotropy and linewidths decrease with increasing labeling position (n) down the lipid chain. Accordingly, in the standard PLPC MLVs, the 5-DSA showed the characteristic spectrum reflecting the local rigidity of the molecule in the sub-headgroup region of the lipid bilayer and the 16-DSA a narrow three line spectrum typical of the central region of the bilayer (Fig. S2). The spectra of the reporter molecule 5-DSA did not show relevant changes upon addition of OHPLPC or HpPLPC. On the other side, the nitroxide at position 16 in the presence of pure OHPLPC and pure HpPLPC became slightly more restricted in motion, in line with previous data [17].

The fact that the spectra of the two reporter positions (5 and 16) in the presence of oxidized species still show the characteristic features observed in normal PLPC bilayers confirms that the spin-labeled probes are properly packed into the bilayer and no dislocation of the lipid chain occurred.

3.2. Effect of lipid peroxidation on the water penetration into lipid bilayers

To obtain information on the effects of lipid peroxidation on water penetration in MLVs, W-band EPR spectra were detected at cryogenic temperature. The capillaries equilibrated at room temperature were shock frozen in liquid nitrogen and then transferred to the pre-cooled W-band cavity at 160 K. This procedure was adopted to provide a snapshot of the polarity and proticity properties of the fluid membrane. One cycle of freezing and thawing was shown not to affect the EPR spectral features, proving that the bilayer integrity is maintained during the W-band measurement (Fig. S3). The A_{zz} and g_{xx} values extracted from the W-band spectra are known to be sensitive indicators for the polarity (electric fields along the NO bond of the nitroxide) and proticity (H-bond formation towards the NO group) character of the nitroxide micro-environment [36].

Fig. 2 shows the comparison of the W-band spectra for the n-DSA and n-DSPPC species investigated. The g_{xx} region of the spectra appears very heterogeneous in the case of the position 16 in the middle of the membrane bilayer, indicating the presence of two populations characterized by different g_{xx} values, as was already previously observed in doxyl spin-labeled lipids in membrane bilayers and protic solvents [37,38]. An even more pronounced heterogeneity is observed in spin-labeled proteins, where the number of components can be up to three [39]. The two nitroxide populations visible in the W-band spectra at low temperatures are interpreted in terms of different H-bonding propensities of the nitroxide population: the lowest g_{xx} corresponds to nitroxides with one H-bond formed with an available H-bond donor, the highest g_{xx} to a population without H-bonds. The H-bond donor for doxyl probes in non-oxidized membranes has been confirmed by ESEEM and ENDOR studies to be a water molecule found in a specific geometry with respect to the nitroxide group [38,40].

For position 5, a broad peak appears in the g_{xx} region, typical for nitroxides in contact with water molecules showing a large g-strain which does not enable to distinguish different populations within the spectral linewidth. Interestingly, no detectable effects in the g_{xx} or in the A_{zz} were observed for the nitroxides close to the membrane headgroups (5-DSA and 5-DSPPC) under any oxidation condition.

On the contrary, the heterogeneous shape of the g_{xx} peak of 16-DSA and 16-DSPPC changed in the presence of HpPLPC and OHPLPC, with the MLVs containing 100% of the oxidized species showing the most relevant changes. The overall movement of the g_{xx} peak towards higher magnetic field correlates with an increase in the A_{zz} value (arrows in Fig. 2), thus indicating a higher polarity and proticity of the nitroxide probes upon lipid oxidation.

The spectra of 16-DSA and 16-DSPPC in different MLVs could be only simulated with two populations of nitroxides characterized by two values of g_{xx} ($g_{xx1} = 2.00863 \pm 0.00002$; $g_{xx2} = 2.00919 \pm 0.00001$) as shown in Fig. 3. The values of the two g_{xxi} were kept constant in the fitting while their ratio was varied.

The fraction corresponding to g_{xx1} is assigned to an H-bonded nitroxide population, while the fraction corresponding to g_{xx2} is assigned to a non H-bonded nitroxide population. In pure PLPC the fraction of the H-bonded water exposed population is around 28% for both DSA and DSPPC spin-labeled moieties (Fig. 4). This fraction slightly increased in the presence of 1:1 PLPC–HpPLPC mixtures (up to 30–35%) and further increased in the case of pure HpPLPC and OHPLPC. The stronger effects were reported by 16-DSA in MLVs formed with pure HpPLPC (67%). Concomitantly, the A_{zz} parameter, which is sensitive to the polarity of the nitroxide micro-environment, increased from 3.28 mT in the pure PLPC to 3.45 mT in the case of the other samples, indicating a general increase in polarity both in the semi and fully oxidized membranes (Table S1). The more distinguishable effects in g_{xx} than in A_{zz} values are a consequence of the fact that the g_{xx} value depends strongly on both polarity and H-bonding, making it a better reporter for the overall changes in the nitroxide micro-environment. Moreover, the composite nature of the g_{xx} peak in the case of the spin labels at positions 16 made it possible to clearly distinguish even subtle changes in the spectral features, which are not visible in the hyperfine lines of the g_{zz} region of the spectrum.

The fits on the spectra of the analogous samples with the reporter spin label at position 5 were performed with a single nitroxide population with a g_{xx} value characterized by a 0.0008 strain which was found to be not affected by the level of oxidation (Fig. S4, Table S1). The plot of the mean g_{xx} values versus A_{zz} is presented in Fig. 4B, showing the effect of HpPLPC and OHPLPC in the water penetration in the central region of the membrane bilayer. The strongest effect is seen for 16-DSA in pure HpPLPC which is found in the same region of the g_{xx} versus A_{zz} plot as the water exposed 5-DSA in pure PLPC (arrows in Fig. 4), indicating the relevant change in the water accessibility in these oxidized MLVs. Similar but less pronounced effects are probed by the 16-DSPPC variants.

3.3. MD simulations of H-bonding to the nitroxide group in oxidized membranes

In the presence of HpPLPC, we observed the most pronounced increase in proticity in the 16-DSA probe. This implies a higher propensity of the spin labels in the center of the bilayer to form H-bonds with nearby H-bond donors. These donors could be nearby water molecules or possibly nearby OOH groups from the oxidized lipids. To disentangle these two possibilities, molecular dynamics simulations were performed with 2 molecules of 16-DSA randomly placed in each leaflet of a bilayer containing 62 molecules each of HpPLPC and PLPC (Fig. 5A). The results of a 200-ns trajectory are shown in Fig. 5B in terms of the number of NO–OOH and NO–water encounters. The encounters of the NO group with the OOH group are much less likely compared to NO–water encounters, indicating that water molecules are statistically much more favored than the oxidized lipids to form H-bonds to the nitroxide group. Based on the MD data, we conclude that the EPR data revealed H-bonds formed prevalently with water molecules, and not with the OOH groups of HpPLPC.

4. Discussion

Unsaturated phospholipids, glycolipids, and cholesterol in cell membranes and other organized systems are prominent targets of oxidant attack. This can result in lipid peroxidation, a degenerative process that is the molecular basis for oxidative stress-related pathologies at a membrane level. Here we address experimentally by W-band EPR the question if lipid peroxidation in MLVs can affect water penetration in the bilayer, as already suggested by MD simulations [9]. We focus on the effects induced in model membranes formed by PLPC by the introduction of the two leading intermediate species in lipid peroxidation, namely HpPLPC and OHPLPC in a 50 to 100% molar percentage.

All model membranes investigated showed spectral features at room temperature in agreement with the normal gradient observed in fluid membranes. To address the possible change in water penetration in the bilayer, we took advantage of W-band spectroscopy at low temperature. First, the higher microwave frequencies provide important

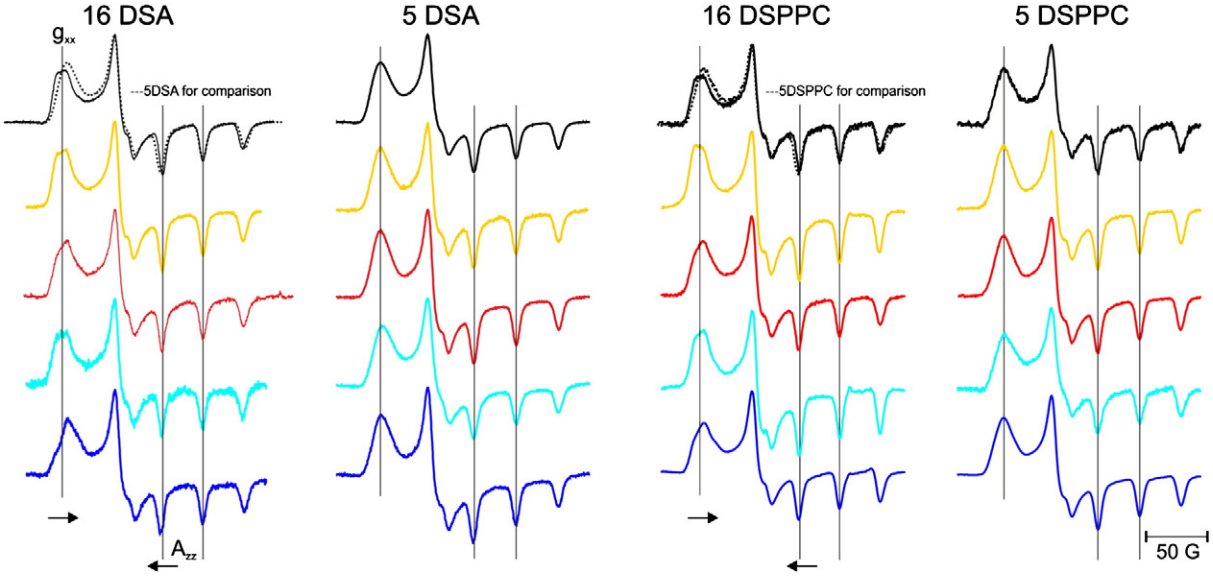

Fig. 2. Low temperature (160 K) W-band spectra of n-DSA and n-DSPPC in different MLVs. Pure PLPC (*black*); pure OHPLPC (*red*); pure HpPLPC (*blue*); OHPLPC/PLPC 1:1 in mol (*yellow*) and HpPLPC/PLPC 1:1 in mol (*cyan*). Arrows highlight the changes in g_{xx} and A_{zz}.

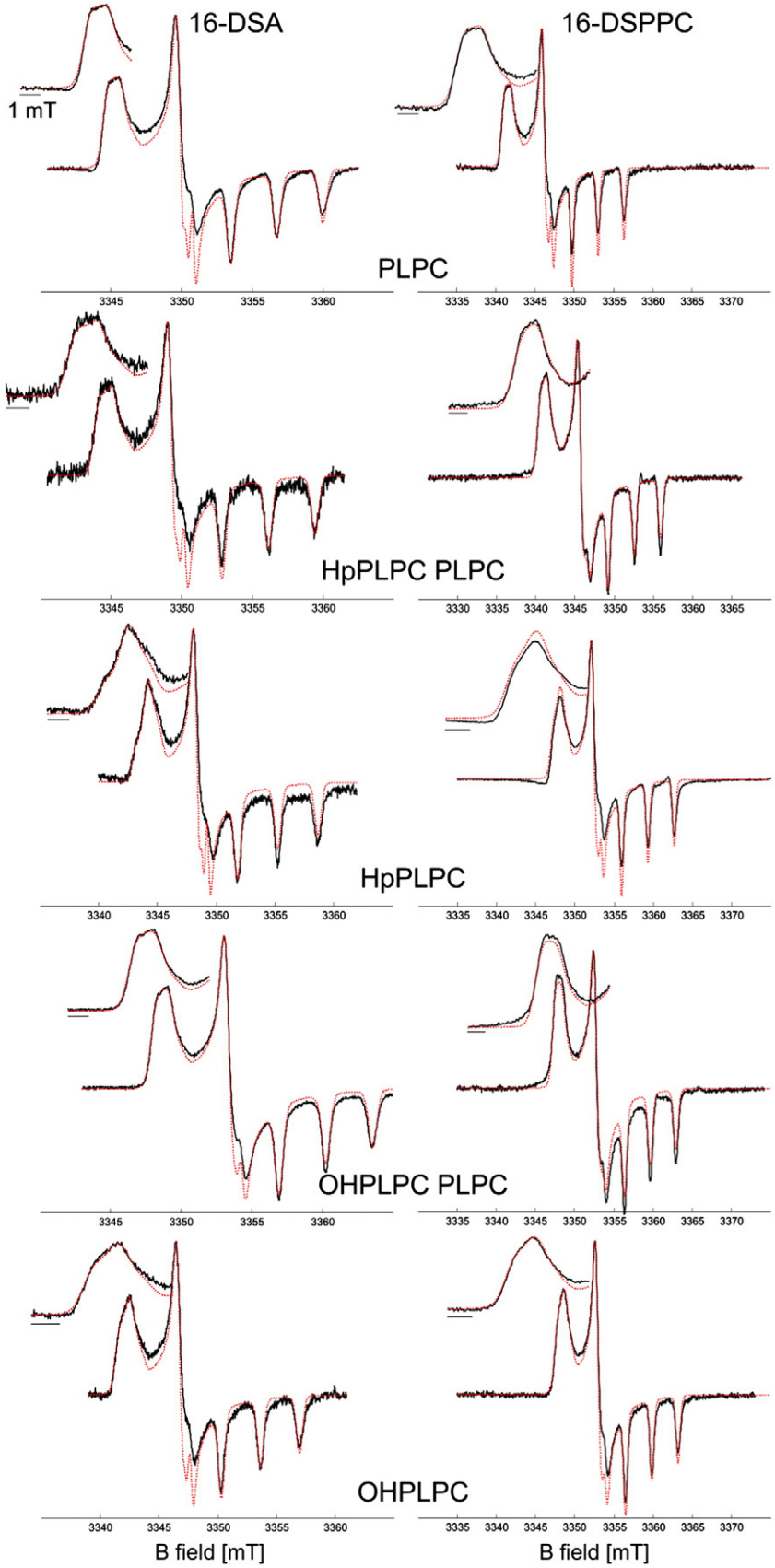

Fig. 3. Fits of the simulated (*red*) to the experimental (*black*) spectra of 16-DSA and 16-DSPPC in different MLVs. The spectra are simulated with two components characterized by different g_{xx} values. The insets show the magnified low field region of the spectra to highlight the heterogeneity of the g_{xx} region.

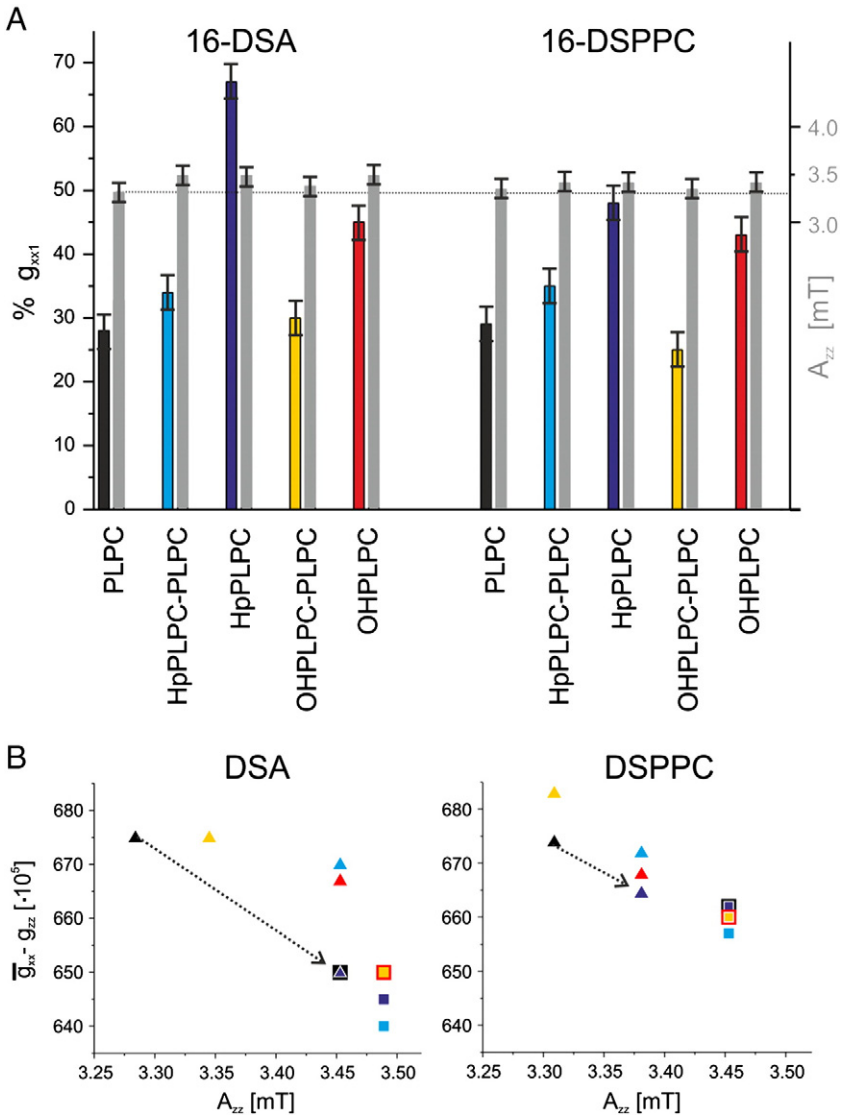

Fig. 4. (A). Fraction (%) of the nitroxide population characterized by the g_{xx1} parameter as obtained from the fits (*colored bars*) and A_{zz} values (*in mT, grey bars*). The estimated error for the g_{xxi} values is ±5E−5, for the fraction is ±2.5%. The estimated error for A_{zz} is ±0.01 mT. (B). Correlation between average g_{xx} and A_{zz} values for 5-DSA (■) and 16-DSA (▲) (left graph) and for 5-DSPPC (■) and 16-DSPPC (▲) (right graph) in different MLVs. The value obtained from the fit of the g_{zz} component (~2.0021–2.0022) has been subtracted from the average g_{xx} value to account for small errors in the B field calibration. The arrows indicate the most relevant change in polarity and proticity as probed by 16-DSA and 16-DSPPC going from pure PLPC to pure HpPLPC. Color code as in panel (A).

advantages with respect to the lower frequency measurements on polarity and proticity determination in terms of spectral resolution [37]. Second, fluid MLVs equilibrated at room temperature are shock frozen in liquid nitrogen for W-band measurements, which can be considered a better method to obtain a snapshot of the membrane physiological conditions than warming the MLVs up to 80 °C to extract the isotropic hyperfine coupling constant at X band. Third, the maximal changes in A_{zz} observed in W band (0.08 for 16-DSPPC and 0.17 mT for 16-DSA, Table S1) would correspond to changes in the order of 0.03–0.05 mT in the isotropic a_0 extracted at 80 °C, which is close to the sensitivity limit of the technique. For these reasons we think that the previous X-band extraction of the isotropic parameter was insensitive to changes in polarity due to lipid peroxidation in model membranes [4].

In this W-band study we found that the nitroxide group located close to the membrane headgroups, thus in a polar environment, is mostly unaffected by the presence of polar hydroxy or hydroperoxide groups. Since the nitroxide already faces a water rich environment in the unoxidized bilayer, it is not sensitive to possibly small changes in water penetration in the bilayer induced by lipid peroxidation.

In contrast, a polarity and proticity increase could be clearly seen for both 16-DSA and 16-DSPPC moieties, with the smallest effects induced by the PLPC–OHPLPC mixture and the most relevant effects induced in the presence of 100% HpPLPC. Of the two nitroxide populations, the one characterized by the lower g_{xx1} value which shows higher propensity to form H-bonds when in contact with H-bond donors increases its relative weight in the OHPLPC/PLPC mixtures and in the MLVs containing 50 or 100% HpPLPC.

Recently, Freed and co-workers suggested that the origin of the H-bonded fraction observed in DOPC and DPPC membranes containing n-PC spin labels (n>7) arises from bent conformations of the spin-labeled lipids in gel and frozen membrane bilayers [41]. The nitroxide moiety in the bent lipid is suggested to be back to the surface region with high water content. Although the results are intriguing, the analysis was performed in membranes in the gel phase (DOPC and DPPC have

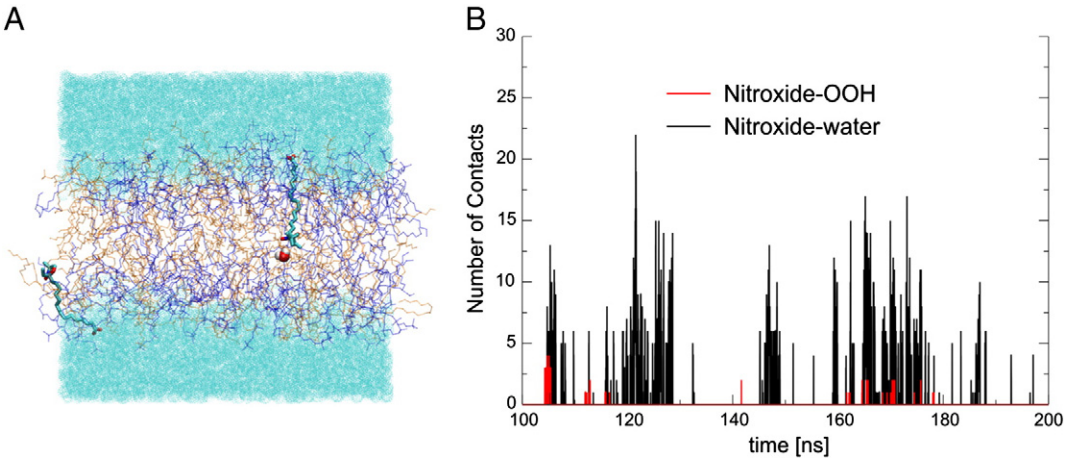

Fig. 5. (A). Snapshot of the MD trajectory (126 ns) showing the HpPLPC (blue) and PLPC (orange) lipids in the membrane bilayer. The two 16-DSA molecules inserted in the two leaflets and the water molecule nearby the nitroxide group of one of the 16-DSA moiety are highlighted. (B) Number of contacts for the last 100 ns of the simulation between the NO group of 16-DSA with the –OOH group of HpPLPC (red lines) and with water molecules (black lines). A contact was counted when the distance between the two moieties was less than 4 Å. Details of the simulation are reported in the Materials and methods section. The probability of NO–water contacts is much higher than that of NO–OOH contacts.

transition temperatures >20 °C) and in the fluid phase things may be different, as the authors also pointed out. Here we performed the W-band experiments by shock freezing the membrane bilayers in the fluid phase (above their transition temperatures) to try to trap the properties of the fluid membranes. Thus, we can assume that the nitroxide groups of the 16-DSA and 16-DSPPC are prevalently in the middle of the membrane bilayer. Although the reporter spin labels may show more affinity to structural defects in membranes, which could be possibly also enhanced by oxidation, the observed increase in H-bonds can be considered a feature of the fluid membrane.

The fact that for the spin labels at position 16 we simultaneously detect an increase of A_{zz} (sensitive mainly to the electric field along the N–O bond) and a decrease of g_{xx} (which is affected both by the polarity and by the H-bonds to the N–O group) allows us to address selectively the pure polarity effects due to charged atoms or electric dipole moments creating an electric field along the NO bond, and the combined H-bonding effects which require an H-donor (usually an OH group). To form an H-bond to the doxyl nitroxide group the OH moiety has to be within 2 Å to the NO group of the label in a specific geometrical arrangement. The same length and orientation of the hydrogen bond to the doxyl probe were found in different solvents and in membranes, indicating that nearly identical hydrogen bonds have been formed regardless of the solvent dielectric constant [38,40]. This strengthens the hypothesis that high field-frequency EPR spectra are exclusively sensitive to formation of specific hydrogen bonds to the NO group and can be used to probe in membrane bilayers the hydrogen-bond network between waters and spin-labeled lipids.

The molecular dynamics simulations performed here in a PLPC–HpPLPC fluid bilayer containing the 16-DSA showed that the molecular encounters between the nitroxide moieties in the middle of the membrane bilayer and the oxidized groups are negligible with respect to those with the water molecules penetrating the bilayer. The MD data thus indicates that the increased H-bond propensity in the oxidized membrane detected by EPR can be mostly explained in terms of an enhanced water penetration, rather than H-bonding between the probe and the oxidized lipid.

Acknowledgements

E.C. thanks Ms. Cecilia Mancazzo for skillful experimental collaboration. E.C. was partially financed by the COST P15 network program of the European Union, which is gratefully acknowledged, and by the Ph.D. research fellowship financed by University of Bari. HK is funded by a Lundbeck Junior Group Leader Fellowhip. Computations were carried out at the SDU node of the Danish Center for Scientific Computing. We thank Luca Monticelli and Tomasz Rog for sharing force field parameters. We thank an anonymous reviewer for the helpful comments on the molecular origin of the H-bond donors.

Appendix A. Supplementary data

Supplementary data to this article can be found online at http://dx.doi.org/10.1016/j.bbamem.2012.09.026.

References

[1] Oxidized phospholipids — their properties and interactions with proteins, Biochim. Biophys. Acta 1818 (2012) 2373–2474.
[2] F.M. Megli, K. Sabatini, EPR studies of phospholipid bilayers after lipoperoxidation. 1. Inner molecular order and fluidity gradient, Chem. Phys. Lipids 125 (2003) 161–172.
[3] F.M. Megli, L. Russo, K. Sabatini, Oxidized phospholipids induce phase separation in lipid vesicles, FEBS Lett. 579 (2005) 4577–4584.
[4] F.M. Megli, L. Russo, E. Conte, Spin labeling EPR studies of the properties of oxidized phospholipid-containing lipid vesicles, Biochim. Biophys. Acta 1788 (2009) 371–379.
[5] K. Sabatini, J.P. Mattila, F.M. Megli, P.K. Kinnunen, Characterization of two oxidatively modified phospholipids in mixed monolayers with DPPC, Biophys. J. 90 (2006) 4488–4499.
[6] M.E. Greenberg, X.M. Li, B.G. Gugiu, X. Gu, J. Qin, R.G. Salomon, S.L. Hazen, The lipid whisker model of the structure of oxidized cell membranes, J. Biol. Chem. 283 (2008) 2385–2396.
[7] H. Khandelia, O.G. Mouritsen, Lipid gymnastics: evidence of complete acyl chain reversal in oxidized phospholipids from molecular simulations, Biophys. J. 96 (2009) 2734–2743.
[8] L. Beranova, L. Cwiklik, P. Jurkiewicz, M. Hof, P. Jungwirth, Oxidation changes physical properties of phospholipid bilayers: fluorescence spectroscopy and molecular simulations, Langmuir 26 (2010) 6140–6144.
[9] J. Wong-Ekkabut, Z. Xu, W. Triampo, I.M. Tang, D.P. Tieleman, L. Monticelli, Effect of lipid peroxidation on the properties of lipid bilayers: a molecular dynamics study, Biophys. J. 93 (2007) 4225–4236.
[10] T. Parasassi, A.M. Giusti, E. Gratton, E. Monaco, M. Raimondi, G. Ravagnan, O. Sapora, Evidence for an increase in water concentration in bilayers after oxidative damage of phospholipids induced by ionizing radiation, Int. J. Radiat. Biol. 65 (1994) 329–334.
[11] R. Volinsky, L. Cwiklik, P. Jurkiewicz, M. Hof, P. Jungwirth, P.K. Kinnunen, Oxidized phosphatidylcholines facilitate phospholipid flip-flop in liposomes, Biophys. J. 101 (2011) 1376–1384.
[12] G. Spiteller, The relation of lipid peroxidation processes with atherogenesis: a new theory on atherogenesis, Mol. Nutr. Food Res. 49 (2005) 999–1013.
[13] E. Niki, Lipid peroxidation: physiological levels and dual biological effects, Free Radic. Biol. Med. 47 (2009) 469–484.
[14] L.J. Sparvero, A.A. Amoscato, P.M. Kochanek, B.R. Pitt, V.E. Kagan, H. Bayir, Mass-spectrometry based oxidative lipidomics and lipid imaging: applications in traumatic brain injury, J. Neurochem. 115 (2010) 1322–1336.
[15] Y.Y. Tyurina, V.A. Tyurin, A.M. Kaynar, V.I. Kapralova, K. Wasserloos, J. Li, M. Mosher, L. Wright, P. Wipf, S. Watkins, B.R. Pitt, V.E. Kagan, Oxidative lipidomics of hyperoxic acute lung injury: mass spectrometric characterization of cardiolipin and phosphatidylserine peroxidation, Am. J. Physiol. Lung Cell. Mol. Physiol. 299 (2010) L73–L85.

[16] R.C. Bruch, W.S. Thayer, Differential effect of lipid peroxidation on membrane fluidity as determined by electron spin resonance probes, Biochim. Biophys. Acta 733 (1983) 216–222.
[17] F.M. Megli, L. Russo, Different oxidized phospholipid molecules unequally affect bilayer packing, Biochim. Biophys. Acta 1778 (2008) 143–152.
[18] W.F. Boss, C.J. Kelley, F.R. Landsberger, A novel synthesis of spin label derivatives of phosphatidylcholine, Anal. Biochem. 64 (1975) 289–292.
[19] J. Eskola, S. Laakso, Bile salt-dependent oxygenation of polyunsaturated phosphatidylcholines by soybean lipoxygenase-1, Biochim. Biophys. Acta, Lipids Lipid Metab. 751 (1983) 305–311.
[20] F.M. Megli, E. Conte, L. Russo, Comparative 5-doxylstearoyllecithin and 3-doxylcholestane EPR spin labeling study of phospholipid bilayer perturbation by different oxidized lecithin species, Biochim. Biophys. Acta 1798 (2010) 1886–1898.
[21] E.G. Bligh, W.J. Dyer, A rapid method of total lipid extraction and purification, Can. J. Biochem. Physiol. 37 (1959) 911–917.
[22] G.R. Nakamura, Microdetermination of phosphorus, Anal. Chem. 24 (1952) 1372.
[23] D. Marsh, A. Watts, P.F. Knowles, Cooperativity of the phase transition in single- and multibilayer lipid vesicles, Biochim. Biophys. Acta 465 (1977) 500–514.
[24] S. Stoll, A. Schweiger, EasySpin, a comprehensive software package for spectral simulation and analysis in EPR, J. Magn. Reson. 178 (2006) 42–55.
[25] O. Berger, O. Edholm, F. Jahnig, Molecular dynamics simulations of a fluid bilayer of dipalmitoylphosphatidylcholine at full hydration, constant pressure, and constant temperature, Biophys. J. 72 (1997) 2002–2013.
[26] L. Stimson, L. Dong, M. Karttunen, A. Wisniewska, M. Dutka, T. Rog, Stearic acid spin labels in lipid bilayers: insight through atomistic simulations, J. Phys. Chem. B 111 (2007) 12447–12453.
[27] H.J.C. Berendsen, J.P.M. Postma, W.F.v. Gunsteren, J. Hermans, Interaction models for water in relation to protein hydration, in: B. Pullman (Ed.), Intermolecular Forces (Jerusalem Symposia), Springer, 1981, pp. 331–342.
[28] H.J.C. Berendsen, D. van der Spoel, R. van Drunen, GROMACS: a message-passing parallel molecular dynamics implementation, Comput. Phys. Commun. 91 (1995) 43–56.
[29] B. Hess, C. Kutzner, D. van der Spoel, E. Lindahl, GROMACS 4: algorithms for highly efficient, load-balanced, and scalable molecular simulation, J. Chem. Theory Comput. 4 (2008) 435–447.
[30] D.V.D. Spoel, E. Lindahl, B. Hess, G. Groenhof, A.E. Mark, H.J.C. Berendsen, GROMACS: fast, flexible, and free, J. Comput. Chem. 26 (2005) 1701–1718.
[31] H. Khandelia, S. Witzke, O.G. Mouritsen, Interaction of salicylate and a terpenoid plant extract with model membranes: reconciling experiments and simulations, Biophys. J. 99 (2010) 3887–3894.
[32] A.R. Leach, Molecular Modelling: Principles and Applications, 2 ed. Pearson Prentice Hall, Harlow, England, 2001.
[33] S. Nose, A molecular dynamics method for simulations in the canonical ensemble, Mol. Phys. 52 (1984) 255–268.
[34] S. Nose, M.L. Klein, Constant pressure molecular-dynamics for molecular systems, Mol. Phys. 50 (1983) 1055–1076.
[35] M. Parrinello, A. Rahman, Polymorphic transitions in single crystals: a new molecular dynamics method, J. Appl. Phys. 52 (1981) 7182–7190.
[36] D. Marsh, Spin-label EPR for determining polarity and proticity in biomolecular assemblies: transmembrane profiles, Appl. Magn. Reson. 37 (2010) 435–454.
[37] D. Kurad, G. Jeschke, D. Marsh, Lipid membrane polarity profiles by high-field EPR, Biophys. J. 85 (2003) 1025–1033.
[38] T.I. Smirnova, A.I. Smirnov, S.V. Paschenko, O.G. Poluektov, Geometry of hydrogen bonds formed by lipid bilayer nitroxide probes: a high-frequency pulsed ENDOR/EPR study, J. Am. Chem. Soc. 129 (2007) 3476–3477.
[39] E. Bordignon, H. Brutlach, L. Urban, K. Hideg, A. Savitsky, A. Schnegg, P. Gast, M. Engelhard, E. Groenen, K. Möbius, H.-J. Steinhoff, Heterogeneity in the nitroxide micro-environment: polarity and proticity effects in spin-labeled proteins studied by multi-frequency EPR, Appl. Magn. Reson. 37 (2010) 391–403.
[40] D.A. Erilov, R. Bartucci, R. Guzzi, A.A. Shubin, A.G. Maryasov, D. Marsh, S.A. Dzuba, L. Sportelli, Water concentration profiles in membranes measured by ESEEM of spin-labeled lipids, J. Phys. Chem. B 109 (2005) 12003–12013.
[41] B. Dzikovski, D. Tipikin, J. Freed, Conformational distributions and hydrogen bonding in gel and frozen lipid bilayers: a high frequency spin-label ESR study, J. Phys. Chem. B 116 (2012) 6694–6706.